Systematic Kinetics of High-Nuclearity Metal Carbonyl Clusters. Exceptional Behavior of $Ru_5C(CO)_{15}$ with P-Donor Nucleophiles

David H. Farrar, Anthony J. Poë,* and Ying Zheng

Contribution from the Lash Miller Chemical Laboratories, University of Toronto, 80 St. George Street, Toronto, Ontario, Canada M5S 1A1

*Received April 4, 1994**

Abstract: The kinetics of reactions of the high-nuclearity carbonyl cluster (HNCC), $Ru_5C(CO)_{15}$, with 21 P-donor nucleophiles, L, to form $Ru_5C(CO)_{14}L$ have been studied. The nucleophiles were chosen such that their electronic ($pK_a' = -2.79$ to 12.20) and steric (Tolman cone angles, $\theta = 101$–$182°$) properties are systematically varied. With 10 smaller nucleophiles ($\theta \leq 133°$) the reactions occur via two well-separated steps: adduct formation and CO-dissociation from the adducts to form the monosubstituted products. The structures of the adducts formed are shown spectroscopically to be closely related to others reported and structurally characterized elsewhere. The rate equations for the two steps are effectively $k_{obs} = k_{+L}[L]$ and $k_{obs} = k_{-CO}$, respectively. With 11 larger nucleophiles ($\theta \geq 136°$) the reaction is a quite different, second-order one-step, process with no spectral evidence for adduct formation being observed. Quantitative analysis of the dependence of the various rate constants on the electronic and steric properties of the nucleophiles or ligands involved shows that adduct formation of this HNCC with the group of smaller nucleophiles is much more facile than any comparable nucleophile-dependent reactions of other metal carbonyls. The rates of loss of CO from the adducts are decreased both by increasing net electron donicity of the ligands involved and by increasing the size of those ligands. The rate constants for the single-step reactions with the group of larger P-donors depend on the latters' electronic and steric properties in a way showing that major expansion of the cluster is required to form the transition states and this is only possible by virtue of an exceptionally high degree of Ru–nucleophile bond-making. The flexibility of the transition state, once formed, is exceptionally low.

Introduction

Transition metal carbido clusters are important in providing specific models of possible intermediates in those Fischer–Tropsch syntheses for which the initial step is C–O bond scission.[1] Pentanuclear high-nuclearity carbonyl clusters (HNCCs) are particularly interesting due to the wide range of skeletal rearrangements that are not only possible but are actually observed.[2,3] This contrasts with the limited range available for M_4 clusters and with the relative rigidity of the octahedral and trigonal prismatic geometries for M_6 clusters.[3] The extreme flexibility and rich chemistry exhibited by pentanuclear HNCCs have made them promising models for surface study.[3] Most of the previous studies of the chemistry of pentanuclear complexes commenced with $Ru_5C(CO)_{15}$, which contains a square-pyramidal Ru_5 core with a partially exposed carbido atom lying 0.11(2) Å beneath the basal plane.[4a] This cluster, and its Os analogue,[4b] are known to form adducts $M_5C(CO)_{15}X$, where X = MeCN, MeOH, F^-, Cl^-, Br^-, I^-, and CO for M = Ru[4a,b] and I^-,[4c] dppe,[4d] and CO[4b] for M = Os. Crystallographic studies of the $Ru_5C(CO)_{15}(NCMe)$[4a] and $Os_5C(CO)_{15}I^-$ [4c] adducts show that they exhibit a wing-tip-bridged butterfly arrangement of metal atoms with a central carbido atom. The cluster core is represented schematically by I, where only the ligands on the bridging metal

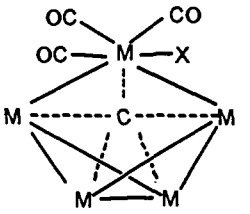

I

atom are shown. The IR spectra of the other adducts suggest[4a] that they have the same structure in solution as $Ru_5C(CO)_{15}(NCMe)$ and $Os_5C(CO)_{15}I^-$. The structural transformation from the square-pyramid to the bridged butterfly geometry upon addition of a pair of electrons can be understood very well in terms of polyhedral skeletal electron pair theory (PSEPT),[5] the former being the most stable geometry for a 74*e* species, while the latter is the most stable for a 76*e* species. Addition of two electrons from the added ligand is compensated for formally by the breaking of one Ru–Ru bond (so the total metal–metal and metal–ligand connectivity in the cluster remains the same). With phosphorus-donor nucleophiles, however, $Ru_5C(CO)_{15}$ was found to form substituted products. The degree of substitution depends on the nature of the nucleophiles, and the substituted products retain the basic structure of the parent cluster.[4a] The intriguing question as to whether these substitution reactions occur via undetected intermediate adducts of the same form as $Ru_5C(CO)_{15}X$ has never been answered, although the fact that reaction with PPh_2Me is faster than that with PPh_3[4a] suggests strongly that the substitution reactions are associative in nature.

* Abstract published in *Advance ACS Abstracts,* June 1, 1994.

(1) Mutterties, E. L.; Stein, J. *Chem. Rev.* **1979**, *79*, 479–490. Brady, R. C.; Petit, R. *J. Am. Chem. Soc.* **1980**, *102*, 6181–6182.

(2) Vargas, M. D.; Nicholls, J. N. *Adv. Inorg. Chem. Radiochem.* **1986**, *30*, 123–222.

(3) Bruce, M. I. *J. Organomet. Chem.* **1990**, *394*, 365–384.

(4) (a) Johnson, B. F. G.; Lewis, J.; Nicholls, J. N.; Puga, J.; Raithby, P. R.; Rosales, M. J.; McPartlin, M.; Clegg, W. *J. Chem. Soc., Dalton Trans.* **1983**, 277–290. (b) Johnson, B. F. G.; Lewis, J.; Nelson, W. J. H.; Nicholls, J. N.; Puga, J.; Raithby, P. R.; Rosales, M. J.; Schröder, M.; Vargas, M. D. *J. Chem. Soc., Dalton Trans.* **1983**, 2447–2457. (c) Jackson, P. F.; Johnson, B. F. G.; Lewis, J.; Nicholls, J. N.; McPartlin, M.; Nelson, W. J. H. *J. Chem. Soc., Chem. Commun.* **1980**, 564–566. (d) Johnson, B. F. G.; Lewis, J.; Raithby, P. R.; Rosales, M. J.; Welch, D. A. *J. Chem. Soc., Dalton Trans.* **1986**, 453–455.

(5) Owen, S. M. *Polyhedron* **1988**, *7*, 253–283. Mingos, D. M. P. In *The Chemistry of Metal Cluster Complexes*; Shriver, D. J., Kaesz, H. D., Adams, R. D., Eds.; VCH Publishers, Inc.: New York, 1990; Chapter 2.

0002-7863/94/1516-6252$04.50/0

The question of whether the exposed carbido atom in a cluster such as $Ru_5C(CO)_{15}$ plays a role in its substitution reactions is also of interest. The exposed carbido atom in $[Fe_5C(CO)_{14}]^{2-}$ is not subject to electrophilic attack, in contrast to that in $[Fe_4C(CO)_{12}]^{2-}$, and this has been associated with particularly low lying, carbon-containing molecular orbitals in the Fe_5C cluster compared with those in lower nuclearity clusters.[6] Steric effects also seems to be very important. The "carbido" carbon atom in the cluster $FeCo_2(CO)_9CCH_2$ is susceptible to nucleophilic attack,[7] but that in $[Fe_2Co(CO)_9CCO]^-$ is not.[8] In view of the general paucity of kinetics studies of HNCCs,[2,9] and of the specific interest of reactions of clusters with exposed carbido atoms, we have studied the reaction kinetics of $Ru_5C(CO)_{15}$ with a wide variety of P-donor nucleophiles. The results reveal that only with smaller nucleophiles (Tolman's cone angle,[10] $\theta \leq 133°$) is the formation of adducts spectroscopically observed, subsequent loss of CO to form substituted products being considerably slower. With larger ($\theta \geq 136°$) nucleophiles no spectral indication of adduct formation is obtained and substitution occurs in a single associative step. Quantitative evaluation[9] of the dependence of the kinetics on the electronic and steric properties of the nucleophiles has led us to conclude that the reactions with the smaller and larger nucleophiles proceed via quite distinct paths, each of which is exceptional in one respect or another.

Experimental Section

Materials. All manipulations were carried out by using standard Schlenk techniques under an atmosphere of oxygen-free N_2. Gases were obtained from Matheson or Canox Ltd. and were research grade. All solvents for synthetic use were reagent grade. Heptane (Caledon) was freshly distilled from Na and bubbled with Argon for 1 h before use. The nucleophiles $PPh(OMe)_2$, $PPh(OEt)_2$, PPh_2H, $PPh_2(OMe)$, $PPh_2(OEt)$, PPh_2Me, $P(NMe_2)_3$, $PPh_2(i\text{-}Pr)$, PPh_2Cy, and $P(t\text{-}Bu)_3$ were used as received (Strem or Aldrich). All other P-donor ligands used in this study were obtained and purified as described elsewhere.[9] The purities of the nucleophiles were checked by ^{31}P-NMR.[9]

$Ru_5C(CO)_{15}$ was prepared from $Ru_6C(CO)_{17}$ by the literature method,[4a] recrystallized at least once from dichloromethane, and characterized by its spectroscopic data: IR spectrum in heptane 2068.0 (vs), 2035.9 (s), 2018.7 (w) cm^{-1}; cf. 2067 (vs), 2034 (s), 2015 (w) cm^{-1} in hexane.[4a] FAB mass spectrum (for M^+): m/e found 937, calcd 937 based on Ru_5 = 505. On TLC plates (silica gel, Baker) $Ru_5C(CO)_{15}$ decomposes quickly to $Ru_3(CO)_{12}$ and some unidentified species. However, the cluster is stable under inert gas in solid form and in solution for a period of a few days. On long-term exposure to air, it decomposes to a black powder in both solid form and in solution.

Instruments. FTIR spectra were obtained by using a Nicolet 10DX FTIR spectrophotometer. UV–vis spectra were measured in thermostated (±0.1 °C) cells in a Cary 2200 or a Hewlett-Packard 8542A diode array spectrophotometer. Stopped-flow experiments were carried out with a Hi-Tech SF-51 apparatus equipped with an SU-40 spectrophotometer unit interfaced with a Hewlett-Packard Series 300 computer and connected with a Hewlett-Packard printer. ^{31}P-NMR spectra were recorded on a Varian XL-200 spectrometer. FAB mass spectra were obtained by using a VG 70-250S mass spectrometer, with a Xenon flux. Matrices used were nitrobenzyl alcohol, thioglycerol, or "magic bullet" matrix.

Product Identification. The monosubstituted complexes $Ru_5C(CO)_{14}L$ (L = PPh_3, $P(p\text{-}MeOC_6H_4)_3$, $P(p\text{-}ClC_6H_4)_3$, $P(p\text{-}CF_3C_6H_4)_3$, $P(NMe_2)_3$, PPh_2Cy, PCy_3, $PPh(OMe)_2$, $PPh(OEt)_2$, and $P(OPh)_3$) were prepared by mixing ca. 1 equiv each of $Ru_5C(CO)_{15}$ and L in small amounts of dichloromethane and stirring under nitrogen until the ν_{CO} band of the parent complex had disappeared. The deep red solutions were then evaporated under vacuum and the products purified by TLC in 50% hexane–dichloromethane. Other $Ru_5C(CO)_{14}L$ complexes (L = etpb,[11] $P(OMe)_3$, $P(OEt)_3$, $P(O\text{-}i\text{-}Pr)_3$, $PPh_2(OMe)$, $PPh_2(OEt)$, PPh_2Me, PPh_2H, $PPh_2(i\text{-}Pr)$, $P(p\text{-}MeC_6H_4)_3$, and $P(t\text{-}Bu)_3$) were prepared in situ by mixing $Ru_5C(CO)_{15}$ with a small molar excess of L in heptane but were not isolated from solution. All products were identified by comparing their FTIR spectra with that of the crystallographically characterized $Ru_5C(CO)_{14}(PPh_3)$:[4a] for example, $Ru_5C(CO)_{14}(PPh_3)$ in heptane, 2087.3 (w), 2056.5 (s), 2046.7 (m), 2025.8 (m), 2015.5 (m), 2001.5 (w) cm^{-1}; and in hexane,[4a] 2087 (w), 2056 (s), 2046 (m), 2025 (m), 2014 (m) cm^{-1}. The cluster $Ru_5C(CO)_{14}(P(p\text{-}MeOC_6H_4)_3)$ was also characterized by single-crystal structure analysis.[12] FTIR spectra for the products obtained in this study are given in Table VIII in the supplementary material. FAB mass spectra (for M^+, m/e) were obtained for the following $Ru_5C(CO)_{14}L$ compounds: L = PPh_3, found 1173, calcd M = 1171; $P(p\text{-}ClC_6H_4)_3$, found 1275, calcd 1275; PCy_3, found 1191, calcd 1190, all calculated values being based on Ru_5 = 505.

Kinetic Studies. All kinetic runs were carried out in the absence of O_2 and under pseudo-first-order conditions by using at least a 10-fold molar excess of nucleophiles. The methods of data acquisition and analysis were exactly as described elsewhere.[9] All the products of the kinetically studied reactions were identified by comparing their IR spectra with those of isolated products (see above).

Results

Reactions with Smaller ($\theta \leq 133°$) P-Donor Nucleophiles. The monosubstitution reactions of $Ru_5C(CO)_{15}$ with 10 relatively small nucleophiles ($\theta \leq 133°$) were all found to proceed via a two-stage process. An immediate color change sequence (red to yellow and then to a deeper red) is always observed. In terms of UV–vis spectroscopic monitoring at a given wavelength this was observed as a fast initial absorbance decrease, followed by a slower absorbance increase. All substituted products, $Ru_5C(CO)_{14}L$, have a higher molar absorptivity than the parent cluster. The IR spectra of the products of the second, slower reaction were identical with those of the separately isolated monosubstituted clusters $Ru_5C(CO)_{14}L$, and the rapid initial color change from red to yellow was also observed during formation of the adducts $Ru_5C(CO)_{15}X$ (X = NCMe, MeOH, F^-, Cl^-, Br^-, I^-, and CO).[4a,b] These changes were quantified by measurements of molar absorptivities for the parent cluster $Ru_5C(CO)_{15}$ (2830 M^{-1} cm^{-1}, in heptane), the known adduct $Ru_5C(CO)_{15}(NCMe)$ (500 M^{-1} cm^{-1}, in MeCN), and a typical monosubstituted product $Ru_5C(CO)_{14}P(p\text{-}MeOC_6H_4)_3$ (5640 M^{-1} cm^{-1}, in heptane), all at 525 nm (the λ_{max} of $Ru_5C(CO)_{15}$ in heptane). The FTIR spectra observed immediately after mixing $Ru_5C(CO)_{15}$ with a molar equivalent of PPh_2H or $P(OPh)_3$ at ~0 °C were as follows: for added PPh_2H in heptane, 2073.6 (m), 2048.3 (vs), 2022.0 (s), 1997.5 (m), 1987.7 (w), 1975.6 (m) cm^{-1}; for added $P(OPh)_3$ in CH_2Cl_2, 2118.6 (w), 2073.5 (m), 2050.4 (vs), 2017.9 (s), 1998.3 (m), 1982.5 (m), 1968.6 (m) cm^{-1}. These can be compared with those for $Ru_5C(CO)_{15}(NCMe)$ in MeCN:[4a] 2106 (w), 2067 (m, sh), 2053 (s), 2042 (m, sh), 2021 (m, sh), 2011 (m) cm^{-1}; and for $Ru_5C(CO)_{16}$ in hexane; 2077 (m), 2057 (s), 2028 (m) cm^{-1}.[4b] The frequencies of the strongest bands decrease slightly in the order X = CO (2057 cm^{-1}) > NCMe (2053 cm^{-1}) > $P(OPh)_3$ (2050 cm^{-1}) > PPh_2H (2048 cm^{-1}).

The rates of the two steps were generally monitored at 25.0 °C by stopped-flow techniques, the difference in rates being sufficiently large for there to be no problem with obtaining precise values of A_∞ for the initial steps. Absorbance changes of ca. 0.003–0.03 for complex concentrations of ca. 5×10^{-6} to 1×10^{-4} M were successfully converted into precise rate constants by the Datapro software. The rates of the first steps for reactions with $PPh_2(OMe)$ and $PPh_2(OEt)$ were not measured. The first steps of the other reactions all showed an increase in k_{obs} with increasing [L], in good accord with eq 1,

$$k_{obs} = a + k_{+L}[L] \qquad (1)$$

even, in some cases, up to quite high values of [L], e.g. 0.63 M for L = $PPh(OEt)_2$. Data for L = $P(OPh)_3$ are shown in Table 1. Values of k_{+L} and a were obtained by a weighted, linear least-squares analysis[9] and are shown in Table 2, together with their standard deviations and the standard errors of each measurement of k_{obs}. The reactions with some of the nucleophiles were studied at other temperatures, and the activation parameters are included in Table 5.

(6) Kolis, J. W.; Basolo, F.; Shriver, D. F. *J. Am. Chem. Soc.* **1982**, *104*, 5626–5630.
(7) Albiez, T.; Vahrenkamp, H. *Angew. Chem., Int. Ed. Engl.* **1987**, *26*, 572–573.
(8) Ching, S.; Shriver, D. F. *J. Am. Chem. Soc.* **1989**, *111*, 3243–3250.
(9) Poë, A. J.; Farrar, D. H.; Zheng, Y. *J. Am. Chem. Soc.* **1992**, *114*, 5146–5152.
(10) Tolman, C. A. *Chem. Rev.* **1977**, *77*, 313–348. Tolman, C. A. *J. Am. Chem. Soc.* **1970**, *92*, 2956–2965.
(11) etpb = 4-ethyl-2,6,7-trioxaphosphabicyclo[2.2.2]octane, $P(OCH_2)_3CEt$.
(12) Farrar, D. H.; Lough, A. J.; Poë, A. J.; Zheng, Y. Unpublished results.

Table 1. Pseudo-First-Order Rate Constants for Reactions of $Ru_5C(CO)_{15}$ with $P(OPh)_3$ in Heptane

T, °C	10^4[P(OPh)$_3$], M	10^2k_{obs}, s^{-1} (first step)	10^3k_{obs}, s^{-1} (second step)
5.1	5.04	9.50	
	9.21	15.7	3.60
	18.4	26.2	2.90
	30.2	39.3	2.20
	46.0	62.6	3.70
17.1	5.04	16.4	12.0
	9.21	26.4	14.0
	18.4	42.8	15.0
	30.2	63.5	15.0
	46.0	91.6	15.0
25.0	22.9	72.8	37.8
	38.2	108	36.7
	76.3	195	37.2
	115	298	45.7
	153	395	37.6
	229	601	37.7
	305	823	38.2
	458	1220	40.6
	611	1630	37.5
	763	1920	34.6
	1145	2790	
	1526	3500	36.9

The values of k_{obs} for the second step were independent of [L] over a wide range, and the averaged values, together with their standard deviations and the standard errors of each value of k_{obs}, are given in Table 3. Activation parameters for some reactions are shown in Table 5. Measurements of the rate of formation of $Ru_5C(CO)_{14}$(etpb) from $Ru_5C(CO)_{15}$(etpb) were complicated by further reaction to form $Ru_5C(CO)_{13}(etpb)_2$. This was not too serious at lower temperatures, where double-exponential analysis of the absorbance changes was possible, but the scatter of the data was still significant. At 25.0 °C, however, no data could be obtained and the value of k_{-CO} had to be estimated by extrapolation of data from two lower temperatures by assuming normal Eyring behavior.

The spectroscopic changes, the nature of the final products, and the facts that the first stage is strictly first order in [L] while the second stage is independent of [L], all show clearly that the first step is adduct formation (eq 2)and the second is CO dissociation (eq 3). The values of a vary

$$Ru_5C(CO)_{15} + L \xrightarrow{k_{+L}} Ru_5C(CO)_{15}L \ (\theta_L \leq 133°) \quad (2)$$

$$Ru_5C(CO)_{15}L \xrightarrow{k_{-CO}} Ru_5C(CO)_{14}L + CO \quad (3)$$

randomly and are often negative, even "significantly" so when their standard deviations are considered. They cannot, therefore, correspond to a CO-dissociative path, and we have to conclude that they generally arise from occasional small systematic errors or statistical accidents that can lead to apparently significant values. However, the adduct formation reactions with etpb and $P(OPh)_3$ do seem to have significant and positive values of a, and it is possible that, for these weakly basic ligands, the values of a represent k_{-L}, the first-order rate constant for the reverse of eq 2. The reactions of these ligands would then involve approach to an equilibrium mixture of $Ru_5C(CO)_{15}$ and $Ru_5C(CO)_{15}L$ with equilibrium constants of ca. 10^3–10^4 M^{-1}, which do not seem unreasonable. In any case the values of a do not have any practical effect in that values of k_{+L} or k_2 (see below) obtained from $k_{obs}/[L]_{max}$ are always essentially the same as those obtained from eq 1 or 5 and fit well to the data analysis presented below.

Reactions with Larger ($\theta \geq 136°$) P-Donor Nucleophiles. Qualitative room temperature FTIR monitoring showed that mixing $Ru_5C(CO)_{15}$ with the larger nucleophiles (apart from the two least basic ones, $P(p\text{-}ClC_6H_4)_3$ and $P(p\text{-}CF_3C_6H_4)_3$, and the largest one, $P(t\text{-}Bu)_3$) results in very rapid formation of the monosubstituted products, $Ru_5C(CO)_{14}L$. Subsequent reactions are much slower and lead to the formation of bis- and tris-substituted products. The reactions with these nucleophiles were therefore studied by stopped-flow techniques. In contrast to reactions with the smaller nucleophiles the formation of the product was accompanied by a steady increase of absorbance over the whole course of the reaction. The data fit well to a single-exponential equation to give the pseudo-first-order rate constants, k_{obs}. Absorbance changes of ca. 0.003–0.2 were obtained for complex concentrations of ca. 1×10^{-5} to 5×10^{-4} M. The products at the end of this step are stable enough to define good values of A_∞, and the FTIR spectra confirm the formation of $Ru_5C(CO)_{14}L$. These reactions therefore occur via a single kinetically detectable substitution pathway, as in eq 4. This was supported by

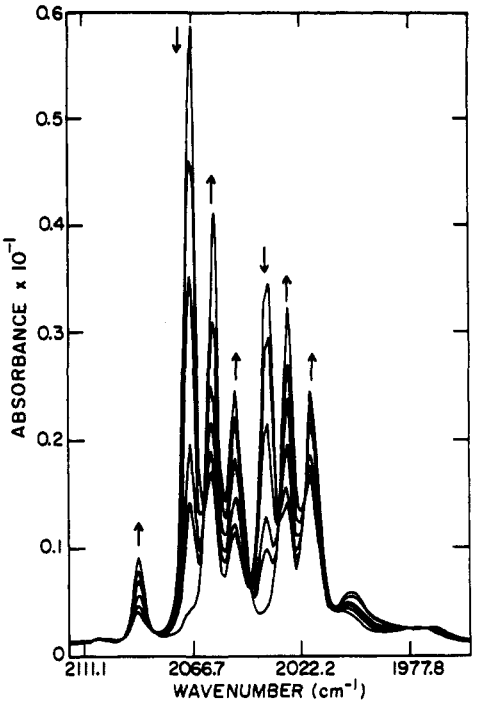

Figure 1. Successive FTIR spectra for reaction of $Ru_5C(CO)_{15}$ (1×10^{-5} M) with $P(p\text{-}ClC_6H_4)_3$ (8.86×10^{-4} M) in heptane at 25.0 °C.

$$Ru_5C(CO)_{15} + L \xrightarrow{k_2} Ru_5C(CO)_{14}L + CO \ (\theta_L \geq 136°) \quad (4)$$

spectroscopic data for the reactions with $P(p\text{-}ClC_6H_4)_3$, $P(p\text{-}CF_3C_6H_4)_3$, and $P(t\text{-}Bu)_3$, which were slow enough to be studied by repetitive FTIR and UV–vis monitorings. Figure 1 shows a series of FTIR spectra recorded during a typical kinetic run. The sharp isosbestic points indicate a clean reaction, and the products are again spectroscopically defined as $Ru_5C(CO)_{14}L$. The absorbance data were successfully analyzed by using a single-exponential fitting program, KORE,[13] to give the values of k_{obs}, and these reactions therefore clearly occur via the path shown in eq 4.

The values of k_{obs} were generally found, by weighted least-squares analyses, to fit well to eq 5 over a wide range of [L]. However, the values

$$k_{obs} = a + k_2[L] \quad (5)$$

of k_{obs} for reactions with PPh_2Me and $P(t\text{-}Bu)_3$, although dependent on [L], were not very reproducible for reasons that were not clear. Values of k_2 and a for all the other nucleophiles are given in Table 4, and activation parameters for reaction with PPh_3 are included in Table 5. Similar remarks are applicable to the values of a in Table 4 as were made above for those in Table 2.

Dependence of the Rate Constants on the Electronic and Steric Properties of the Nucleophiles. (a) General Considerations. It is obvious that the sizes of the P-donor nucleophiles play a dominating role in determining the reaction paths. The contribution of the steric and electronic properties of the nucleophiles to the rates of each second-order path can be assessed by using eq 6.[9] The coefficient β reflects the degree

$$\log k_{+L} = \alpha + \beta(pK_a' + 4) + \gamma(\theta - \theta_{th})\lambda \quad (6)$$

of metal–phosphorus bond-making in the transition state of the second-order reaction.[14] θ_{th} is the steric threshold such that there is no steric effect when the cone angles of the nucleophiles are less than θ_{th} and the

(13) Swain, C. G.; Swain, M. S.; Berg, L. F. *J. Chem. Inf. Comput. Sci.* **1980**, *20*, 47–51.

(14) Poë, A. J. *Pure Appl. Chem.* **1988**, *60*, 1209–1217.

Table 2. Second-Order Rate Constants for the Adduct Formation Reactions of $Ru_5C(CO)_{15}$ with Nucleophiles L ($\theta \leq 130°$), in Heptane (Studied by Stopped-Flow Techniques, [Complex] = 5×10^{-6} to 1×10^{-4} M)

L (no.[a])	pK_a' [b]	θ, deg	T, °C	10^4[L], M	N[c]	a, s^{-1}	k_{+L}, M^{-1} s1–1	$\sigma(k_{obs})$, %[d]
etpb (1)	–0.30	101	5.7	2.15–26.9	3	$(8.78 \pm 3.36) \times 10^{-2}$	$(2.03 \pm 0.07) \times 10^3$	
			13.3	2.58–32.2	4	$(3.73 \pm 0.55) \times 10^{-1}$	$(2.44 \pm 0.10) \times 10^3$	3.5
			21.1	2.58–6.44	3	$(9.12 \pm 0.38) \times 10^{-1}$	$(2.71 \pm 0.29) \times 10^3$	
			25.0				$(3.05 \pm 0.11) \times 10^3$ [e]	
$P(OMe)_3$ (2)	0.83	107	25.0	3.27–8.71	3	$(-3.93 \pm .4.52) \times 10^{-1}$	$(1.54 \pm 0.10) \times 10^4$	4.4
$P(OEt)_3$ (3)	1.64	109	25.0	0.272–6.39	3	$(1.50 \pm 0.70) \times 10^{-1}$	$(9.20 \pm 1.32) \times 10^3$	9.4
$PPh(OMe)_2$ (4)	1.48	120	6.5	2.94–11.1	4	$(-6.7 \pm 10.15) \times 10^{-2}$	$(3.05 \pm 0.14) \times 10^3$	
			13.2	2.94–8.82	3	$(-1.42 \pm 0.80) \times 10^{-1}$	$(3.75 \pm 0.23) \times 10^3$	4.5
			25.0	2.94–8.82	3	$(-2.93 \pm 0.09) \times 10^{-1}$	$(6.51 \pm 0.35) \times 10^3$	
$PPh(OEt)_2$ (5)	1.99	121	14.4	6.17–2205	5	$(6.41 \pm 2.15) \times 10^{-2}$	$(4.86 \pm 0.17) \times 10^2$	
			25.0	10.6–6293	13	$(-4.19 \pm 4.78) \times 10^{-2}$	$(9.76 \pm 0.26) \times 10^2$	5.2
			34.8	8.82–26.5	3	$(-1.79 \pm 18) \times 10^{-2}$	$(1.14 \pm 0.08) \times 10^3$	
PPh_2H (6)	0.52	126	25.0	9.01–18.0	2		$(1.70 \pm 0.16) \times 10^3$ [f]	
$P(OPh)_3$ (7)	–2.79	128	5.1	5.04–46.0	5	$(3.50 \pm 0.60) \times 10^{-2}$	$(1.24 \pm 0.05) \times 10^2$	
			17.1	5.04–46.0	5	$(7.00 \pm 0.70) \times 10^{-2}$	$(1.90 \pm 0.08) \times 10^2$	4.5
			25.0	22.89–1526	12	$(1.44 \pm 0.32) \times 10^{-1}$	$(2.49 \pm 0.04) \times 10^2$	
$P(O\text{-}i\text{-}Pr)_3$ (8)	3.38	130	25.0	1.41–17.6	3	$(1.78 \pm 1.45) \times 10^{-2}$	$(3.57 \pm 0.06) \times 10^3$	3.0

[a] Nucleophile number. This numbering is used in the figures. [b] See text for definition. [c] Number of individual determinations of k_{obs}; $k_{obs} = a + k_{+L}[L]$. Each k_{obs} was obtained by fitting the averaged data of four to eight stopped-flow runs. [d] Standard error of an individual determination of k_{obs} obtained, where possible, by pooling all data for a given nucleophile at all temperatures and then adjusting according to the number of degrees of freedom (ref 9). [e] Obtained from the activation parameters. [f] Average of the two values of $k_{obs}/[L]$ obtained; the uncertainty is from the spread of these values.

Table 3. Kinetic Data for the CO-Dissociation Reactions of the Adducts $Ru_5C(CO)_{15}L$ (L, $\theta \leq 133°$) in Heptane (Studied by Stopped-Flow Techniques Unless Otherwise Indicated; [Complex] = 5×10^{-6} to 1×10^{-4} M)

L (no.[a])	$\delta(^{13}CO)$, ppm	T, °C	10^4[L], M	N[b]	k_{-CO},[c] s^{-1}	$\sigma(k_{obs})$,[d] %
etpb (1)	2.60	5.7	2.15–26.9	3	$(4.07 \pm 0.81) \times 10^{-2}$	16
		13.3	2.58–32.2	3	$(9.13 \pm 1.04) \times 10^{-2}$	
		25.0			~0.4[e]	
$P(OMe)_3$ (2)	3.18	25.0	3.27–8.71	3	$(2.46 \pm 0.07) \times 10^{-1}$	2.8
$P(OEt)_3$ (3)	3.61	16.5	348–1550	2	$(1.40 \pm 0.15) \times 10^{-2}$	
		25.0	0.272–6.79	3	$(3.98 \pm 0.44) \times 10^{-2}$	11
		36.5	463–1550	3	$(7.16 \pm 0.78(\times 10^{-2}$	
$PPh(OMe)_2$ (4)	3.48	6.5	2.94–11.1	4	$(2.10 \pm 0.07) \times 10^{-2}$	
		13.2	2.94–8.82	3	$(3.87 \pm 0.12) \times 10^{-2}$	3.2
		25.0	2.94–8.82	3	$(1.13 \pm 0.04) \times 10^{-1}$	
$PPh(OEt)_2$ (5)	4.04	14.4	6.17–39.7	3	$(1.06 \pm 0.01) \times 10^{-2}$	
		25.0	2.72–44.1	5	$(2.68 \pm 0.03) \times 10^{-2}$	1.1
		34.8	8.82–26.5	3	$(6.86 \pm 0.07) \times 10^{-2}$	
PPh_2H (6)	3.93	25.0	9.01–18.0	2	$(2.99 \pm 0.05) \times 10^{-2}$ [f]	
$P(OPh)_3$ (7)	1.69	5.1	5.04–46.0	4	$(3.10 \pm 0.19) \times 10^{-3}$	
		17.1	5.04–46.0	5	$(1.42 \pm 0.08) \times 10^{-2}$	
		25.0[g]	3.74–1526	18	$(3.79 \pm 0.23) \times 10^{-2}$	6.2
		36.5	152–600	2	$(9.83 \pm 0.62) \times 10^{-2}$	
$P(O\text{-}i\text{-}Pr)_3$ (8)	3.90	25.0	1.41–5.86	2	$(4.57 \pm 0.15) \times 10^{-3}$	
		35.3	318–1250	3	$(9.81 \pm 0.08) \times 10^{-3}$	5.0
		49.8	632–1550	4	$(2.68 \pm 0.03) \times 10^{-2}$	
$PPh_2(OMe)$ (9)[h,i]	3.96	25.0	1.70–7.97	6	$(3.81 \pm 0.22) \times 10^{-2}$	5.8
$PPh_2(OEt)$ (10)[h,j]	4.27	15.4	1.39–22.2	7	$(2.28 \pm 0.05) \times 10^{-3}$	
		25.0	0.56–3.40	7	$(7.35 \pm 0.16) \times 10^{-3}$	
		35.0	1.04–77.0	9	$(2.24 \pm 0.05) \times 10^{-2}$	2.2
		48.2	1.85–52.8	8	$(6.78 \pm 0.15) \times 10^{-2}$	

[a] Numbering of ligand L for use in Figure 3. [b] N represents the number of individual k_{obs} determinations obtained from the different solutions of L used. [c] Values of k_{-CO} at each temperature are averages of the values of k_{obs} for different concentrations of nucleophiles. In the cases of studies made by stopped-flow techniques each value of k_{obs} was obtained from averaged data for two or three stopped-flow runs at a given [L]. [d] Standard error of an individual determination of k_{obs} obtained, where possible, by pooling all data for a given nucleophile at all temperatures and then adjusting according to the number of degrees of freedom (ref 9). [e] Calculated from the activation parameters. [f] Average of the two values of k_{obs} obtained; the uncertainty is from the spread of the values. [g] Data were obtained from both conventional UV–vis spectroscopy and stopped-flow studies. [h] Studied by conventional UV–vis techniques. [i] $\theta = 132°$. [j] $\theta = 133°$.

"switching parameter", λ, is 0.[15] The existence of reactions, below a steric threshold, that show no steric effects at all in spite of the congested array of carbonyl ligands around a metal or cluster of metal atoms has led us to suggest[9] that associative reactions of this type might involve what is essentially an isomerization of the carbonyl complex that is triggered by the approach of the nucleophiles. These reactive isomers are formed by opening up the original cluster so as to create a rather well-defined space which makes approach of smaller nucleophiles possible without steric hindrance. The constant size of the space is related to the value of θ_{th}. When the nucleophile cone angles are $>\theta_{th}$, the isomer cannot accommodate the nucleophiles without steric repulsion, and the difficulty of this process is quantitatively expressed by the (negative) value of γ; that is, γ is a measure of the flexibility of the isomeric form of the cluster in the transition state, the less the flexibility the more negative the value of γ.[16]

Equation 6 allows the value of α ($=\log k_{+L}^{\circ} = \log k_{+L} - \beta(pK_a' + 4)$ when $\theta < \theta_{th}$) to be taken as a measure of the standard reactivity, SR, of the carbonyl complex as defined by the value of log k_{+L} for reaction with a hypothetical, small ($\theta < \theta_{th}$), and weakly basic ($pK_a' = -4$)

(15) Liu, H.-Y.; Eriks, K.; Prock, A.; Giering, W. P. *Organometallics* **1990**, *9*, 1758–1766 and references therein.

(16) An alternative or additional reason for the negative values of γ could be that steric repulsions prevent as close an approach of the nucleophiles with $\theta > \theta_{th}$; that is, the extent of bond-making would be decreased. This would result in lower values of β for these nucleophiles, and no clear data to that effect have been found. However, if this is a contributing factor, it would mean that the value of γ would provide an upper limit to the flexibility of the transition-state isomer, total inflexibility inevitably leading to longer metal to nucleophile bonds.

Table 4. Second-Order Rate Constants for the Reactions of $Ru_5C(CO)_{15}$ with Nucleophiles L ($\theta \geq 145°$), in Heptane (Studied by Stopped-Flow Techniques at 25 °C Unless Otherwise Specified; [Complex] = 1×10^{-5} to 5×10^{-4} M)

L (no.[a])	pK_a' [b]	θ, deg	10^4[L], M	N[c]	a, s^{-1}	k_2, M^{-1} s^{-1}	$\sigma(k_{obs})$, %[d]
P(*p*-MeOC$_6$H$_4$)$_3$ (11)	5.13	145	1.21–3.01	2		$(7.01 \pm 0.25) \times 10^2$ [e]	
P(*p*-MeC$_6$H$_4$)$_3$ (12)	4.46	145	3.04–38.0	3	-0.13 ± 0.01	$(7.35 \pm 0.26) \times 10^2$	4.3
PPh$_3$ (13)	3.28	145	7.41–64.3	6	$(-6.75 \pm 0.39) \times 10^{-2}$	$(1.38 \pm 0.04) \times 10^2$	5.6
			3.66–22.9	5[f]	$(-8.33 \pm 16.9) \times 10^{-4}$	$(5.12 \pm 0.25) \times 10$	6.0
P(*p*-ClC$_6$H$_4$)$_3$ (14)	0.87	145	4.43–10.3	4[g]	$(9.36 \pm 10.16) \times 10^{-5}$	3.36 ± 0.15	2.9
P(*p*-CF$_3$C$_6$H$_4$)$_3$ (15)	−1.39	145	13.0–149	4[g]	$(-6.41 \pm 1.14) \times 10^{-5}$	$(1.64 \pm 0.06) \times 10^{-1}$	4.7
PPh$_2$(*i*-Pr) (16)	4.90	150	69.3–169	4	$(-3.04 \pm 1.27) \times 10^{-1}$	$(3.42 \pm 0.15) \times 10^2$	2.9
PPh$_2$Cy (17)	5.87	153	1.74–8.70	4	$(4.82 \pm 9.51) \times 10^{-3}$	$(2.97 \pm 0.31) \times 10^2$	10
P(NMe$_2$)$_3$ (18)	8.20	157	19.0–1436	7	1.00 ± 0.15	$(6.04 \pm 0.31) \times 10^2$	8.3
PCy$_3$ (19)	11.26	170	56.6–196	3	$(-3.68 \pm 334) \times 10^{-4}$	$(4.11 \pm 0.41) \times 10$	6.9

[a] Nucleophile number. This numbering is used in the figures. [b] See text for definition. [c] Number of individual determinations of k_{obs}; $k_{obs} = a + k_2[L]$. Each k_{obs} was obtained by fitting the averaged data for four to eight stopped-flow runs, unless otherwise specified. [d] Standard error of an individual determination of k_{obs}. [e] Average of the two values of $k_{obs}/[L]$ obtained; the uncertainty is from the spread of these values. [f] At 5.9 °C. [g] Studied by FTIR spectroscopy.

Table 5. Activation Parameters for Reactions of $Ru_5C(CO)_{15}$ with L or of $Ru_5C(CO)_{15}L$

L	N[a]	$\Delta H^{\ddagger}$, kcal mol^{-1}	$\Delta S^{\ddagger}$, cal K^{-1} mol^{-1}
		Adduct Formation	
etpb	3	2.88 ± 0.89	-32.9 ± 3.2
P(OPh)$_3$	3	5.22 ± 0.35	-30.1 ± 1.2
PPh(OMe)$_2$	3	6.24 ± 0.72	-20.2 ± 2.5
PPh(OEt)$_2$	3	8.37 ± 2.82	-16.9 ± 9.5
		CO-Dissociation	
etpb	2[b]	~19	~ +3
P(OEt)$_3$	3	13.7 ± 3.3	-19 ± 11
PPh(OMe)$_2$	3	14.5 ± 0.4	-14.2 ± 1.5
PPh(OEt)$_2$	3	15.4 ± 0.7	-13.9 ± 2.3
P(OPh)$_3$	4	18.5 ± 1.0	-3.4 ± 3.5
P(O-*i*-Pr)$_3$	3	13.0 ± 0.2	-25.5 ± 0.5
PPh$_2$(OEt)	4	18.5 ± 0.8	-6.3 ± 2.5
		Concerted Substitution[c]	
PPh$_3$	2[d]	8.01 ± 0.68	-21.9 ± 2.3

[a] *N* represents the number of temperatures at which the reaction was studied, and the values of the first- or second-order rate constants were the average k_{-CO}, or k_{+L} or $k_2 = (k_{obs} - a)/[L]$, values, unless otherwise indicated. The activation parameters and their uncertainties were obtained by linear least-squares analysis of the dependence of ln (k/T) on $1/T$, where each value of ln (k/T) was weighted according to the variance of the rate constant at each temperature. [b] In this case data were available at only two temperatures; the activation parameters for this ligand were obtained by using the six individual k_{obs} values instead of the averaged k_{-CO} values at each temperature. [c] Only simple second-order rate constants were obtained with no evidence for formation of intermediates. [d] The activation parameters for this ligand were calculated by using the two available values of ln (k_2/T), and the uncertainties were obtained by conventional error propagation rules based on the standard deviations of the k_2 values at the two temperatures studied (Table 3).

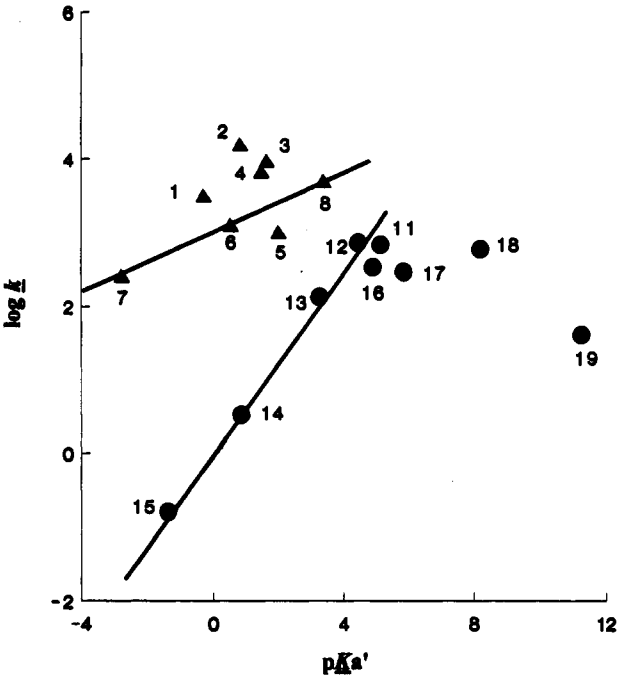

Figure 2. Dependence of log k (log k_{+L} (▲) or log k_2 (●)) on pK_a'. Nucleophile numbering is taken from Tables 2 and 4. Data for nucleophiles 6–8 have been adjusted to what they would have been for a common value of θ (128°) by using the value of γ (−0.068 deg^{-1}) from Table 6. Nucleophiles 11–15 are isosteric (θ = 145°).

nucleophile.[14] If the energy released by bond-making to this nucleophile is small, the value of SR will be close to the intrinsic reactivity, IR, of the carbonyl involved, i.e. to the energy required to generate the transition-state isomer without any assistance from metal–nucleophile bond-making. This will be the situation when β is very small.

The pK_a' values used (Table 2) are not simply the experimental pK_a values for deprotonation in aqueous solution found[17] from acid–base titration. This is because these pK_a values appear to vary[15] with the size of the P-donor ligands due to hydration of the phosphonium cations involved. This phenomenon will not apply to reactions in nonpolar solvents, and our pK_a' values are related directly to the χ_d values derived by Giering et al.[15] but with an appropriate factor introduced to allow for the change of units. This has the desirable feature[14] of leading to dimensionless values of β.

(b) Stereoelectronic Analysis of Data for Adduct Formation by Smaller Nucleophiles. A plot of log k_{+L} vs pK_a' for the smaller nucleophiles, 1–8, is shown in Figure 2. The line drawn through the nearly isosteric nucleophiles 6–8 ($\theta = 128 \pm 2°$) provides an initial indication of the electronic effect, β = 0.2. The other nucleophiles have $\theta \leq 121°$, and data for all but one lie above the line and suggest the existence of a steric effect. The value of k_{+L} for PPh(OEt)$_2$ is almost 10 times slower than that for PPh(OMe)$_2$ (Table 2), which is slightly less basic and has a very similar cone angle. Values of log k_{+L} for the seven nucleophiles 1–4 and 6–8 give a good fit to eq 6, as shown in Table 6 and by the steric profile in Figure 3. The fit to eq 6 is obtained by the use of a multilinear least-squares program that requires initial input of values of θ_{th}. The best value of θ_{th}, 117°, and of the other parameters, is obtained by varying θ_{th} until a minimum in the RMSD (Table 6) is obtained. Thus, values of θ_{th} (RMSD) are ≤101° (0.198), 110° (0.152), 114° (0.139), *117° (0.134)*, 118° (0.137), 119° (0.143), 125° (0.199). The values of k_{+L} for the reactions of the smaller nucleophiles etpb, P(OMe)$_3$, and P(OEt)$_3$, when calculated from the values of β and γ obtained only from the log k_{+L} data for nucleophiles with $\theta > 117°$, are 17, 2.3, and 4.2 times larger, respectively, than the observed ones. The existence of the steric threshold therefore rests largely but strongly on the value of k_{+L} for etpb.

The deviation of the data for PPh(OEt)$_2$ from the well-defined trend (R = 0.969) shown by the other seven nucleophiles is statistically significant (ca. 6 times the value of the RMSD), although the reason for it is not clear. Impurity in the nucleophile would have to be enormous to account for a 10-fold decrease in rates, and the cone angle would have to be ca. 15° higher in order for the data to fit to the steric profile in Figure 3. In that case, the cone angle of PPh(OMe)$_2$ would be expected to be larger too, and one "outlier" would have been replaced by another. Occurrence

(17) Streuli, C. A. *Anal. Chem.* **1959**, *31*, 1652–1655; **1960**, *32*, 985–989. Henderson, W. A.; Streuli, C. A. *J. Am. Chem. Soc.* **1960**, *82*, 5791–5794. Allman, T.; Goel, R. G. *Can. J. Chem.* **1982**, *60*, 716–722.

Table 6. Characteristic Kinetic Parameters for Some Ruthenium Carbonyl Clusters at 25.0 °C[a]

θ_{th}, deg	SR	β	γ, deg^{-1}	R	RMSD[b]	RMSD[c]/Δlog k
		For Adduct Formatin with $Ru_5C(CO)_{15}$ by Smaller Nucleophiles ($\theta \leq 130°$)				
117[d]	2.86 ± 0.18	0.214 ± 0.038	−0.068 ± 0.013	0.969	0.134	0.074
≤120[d,e]	≥2.68[f]	0.209 ± 0.001	−0.066 ± 0.000	0.999	0.002	0.001
		For CO-Dissociation from $Ru_5C(CO)_{15}L$ ($\theta \leq 133$ °C)				
≤101	0.064 ± 0.555[g]	−0.20 ± 0.17[h]	−0.038 ± 0.012	0.840	0.310	0.160
		For Concerted Substitution[i] of $Ru_5C(CO)_{15}$ with Larger Nucleophiles ($\theta \geq 145°$)				
148	−2.30 ± 0.13	0.592 ± 0.024	−0.233 ± 0.012	0.995	0.118	0.032
		For Concerted Substitution of $Ru_6C(CO)_{17}$[j]				
119	1.51 ± 0.26	0.41 ± 0.04	−0.20 ± 0.01	0.986	0.41	0.041
		For Concerted Substitution of $Ru_3(CO)_{12}$ with Smaller Nucleophiles ($\theta \leq 136°$)				
120[k]	−3.4 ± 0.2	0.15 ± 0.03	−0.04 ± 0.01	0.921	0.18	0.10
120[l]	−3.4 ± 0.2	0.15 ± 0.02	−0.03 ± 0.01	0.955	0.25	0.12
		For Concerted Substitution of $Ru_3(CO)_{12}$ with Larger Nucleophiles ($\theta = 145°$)[m]				
		0.347 ± 0.013		0.977	0.059	0.027

[a] Parameters for a selection of other metal carbonyls are given in ref 9. Reactions are in heptane unless otherwise indicated. [b] Root mean square deviation. [c] Ratio of RMSD to the range (Δlog k) of log k values obtained. When the rate constants are very dependent on pK_a' (high β values) and/or θ (large negative γ values), the RMSD values will be expected to be high because of larger effects of any uncertainties in the values of pk_a' and θ, and this ratio takes this into account in indicating the goodness of fit. [d] Omitting data for $PPh(OEt)_2$ (see text). [e] Omitting data for $\theta \leq 120°$ (i.e. $<\theta_{th}$). [f] Since all nucleophiles have $\theta \geq \theta_{th}$, only a lower limit of SR can be estimated, and this is the calculated value of log $k_{+L}°$ (=log $k_{+L} - \beta$(pk_a' + 4)) for the smallest nucleophile ($PPh(OMe)_2$) used in this analysis. This number allows the calculation of expected values of log k_{+L} for smaller nucleophiles when it is assumed that there is no steric threshold (see text). [g] This is the value of log k_{-CO} at $\delta(^{13}CO) = 0$. [h] The electronic parameter for the ligands, L, in the adducts is $\delta(^{13}CO)$, so the units of β are ppm^{-1}. However, a dimensionless value of β (0.10 ± 0.08), comparable with the other values, can be obtained by division of β in ppm^{-1} by 2 (see text). [i] Concerted substitution, here and elsewhere, means that only a simple second-order rate constant is obtained; that is, there is no evidence for formation of any intermediates. [j] See ref 9. [k] In decalin. Data from ref 27. Values of β and γ are appropriate to the temperature (51.6 °C) at which measurements were made, but the value of SR was adjusted to 25 °C by use of the values of $\Delta H_2^{\ddagger}$ for reaction with etpb ($\theta < \theta_{th}$). [l] Reactions in chlorobenzene at 51.6 °C (data from ref 27), but SR was adjusted to 25 °C in the way indicated in footnote *k*. [m] Reactions in chlorobenzene with only the isosteric nucleophiles (p-$XC_6H_4)_3P$ (X = CF_3, Cl, F, H, Me, and OMe), so no values of SR or γ are available. Data from ref 27. High values of [L] are necessary to obtain k_2 because of the significant value of k_{-CO} for dissociative reactions of this cluster. Solubility limitations for these nucleophiles in decalin necessitated the use of an aromatic solvent.

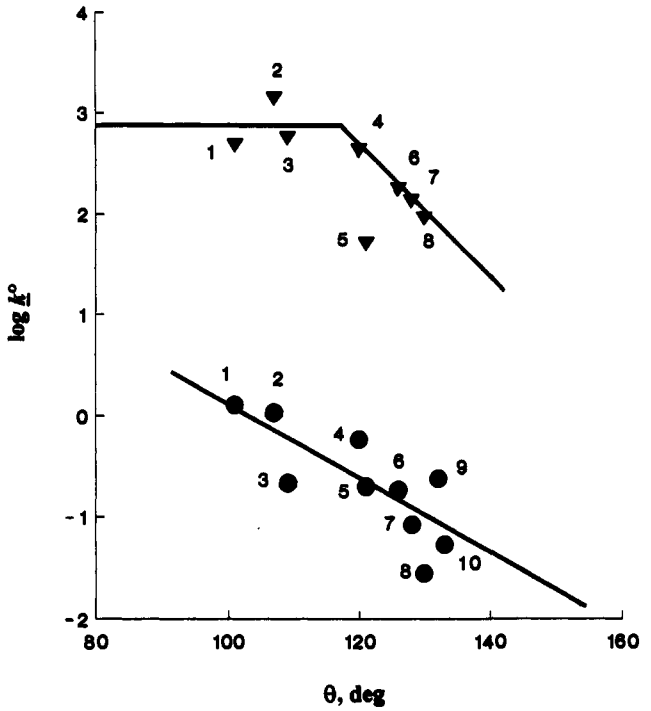

Figure 3. Steric profiles for adduct formation (log $k°$ = log $k_{+L}°$ = log $k_{+L} - \beta$(pK_a' + 4), ▼) and CO-dissociation from the adducts (log $k°$ = log $k_{-CO}°$ = log $k_{-CO} - \beta\delta(^{13}CO)$, ●) obtained by using the parameters in Table 6.

of such outliers is not common but is not unknown[18] in kinetic correlations of this sort where all but one of the data points can give a statistically good fit to a trend. The nucleophiles concerned are not always the same and the absence of a consistent pattern of deviant behavior makes explanations difficult.

(18) Moreno, C.; Delgado, S.; Macazaga, M. J. *Organometallics* **1991**, *10*, 1124–1130. Beringhelli, T.; D'Alphonso, G.; Minoja, A. P.; Freni, M. *Inorg. Chem.* **1991**, *30*, 2757–2763.

(c) Stereoelectronic Analysis of Data for CO-Dissociation from the Adducts. Systematic studies of CO-dissociation reactions are not very common but, where suitable sets of data are available, they are found to be analyzable according to eq 7,[19-21] which is analogous to eq 6. For

$$\log k_{-CO} = \alpha + \beta\delta(^{13}CO) + \gamma(\theta - \theta_{th})\lambda \qquad (7)$$

reactions dependent on the nature of *substituents* it is necessary to take into account the fact that, unlike associative reactions in which the π acidity of the nucleophiles does not appear to be important,[14,22] it must be expected that the π acidity of substituents probably is important. For this reason the electronic parameter used in eq 7 is $\delta(^{13}CO)$, the chemical shift in parts per million of ^{13}CO in $Ni(CO)_3L$ relative to that in $Ni(CO)_4$.[23] The value of β is now in units of inverse parts per million, but it can be converted to dimensionless values as follows. There is a reasonable correlation between the pK_a' and $\delta(^{13}CO)$ values *for the ligands used here*, as shown in eq 8.

$$pK_a' = -(5.66 \pm 1.18) + (1.95 \pm 0.03)\delta(^{13}CO) \qquad (8)$$

$$R = 0.902, \quad \text{RMSD} = \pm 0.704$$

Hence the value of β in inverse parts per million simply has to be divided by 2 to convert it to a dimensionless value that is more comparable with the β values for the adduct formation reactions, so that electronic effects on the two types of reactions can be more meaningfully compared.

Values of θ_{th} define the substituent cone angle above which steric effects become apparent, and their magnitude and direction are provided by the value of γ. Steric effects can show up in the ground and transition states of the complexes, unlike the simpler situation for associative reactions, and it is the difference between the two effects that governs the steric parameters derived from eq 7.[21]

The value of α does not have the same significance as α (=SR) in eq 6 because of the different units of the electronic parameters. In eq 7 it

(19) Chen, L.; Poë, A. J. *Inorg. Chem.* **1989**, *28*, 3641–3647.
(20) Brodie, N. M. J. Ph.D. Thesis, University of Toronto, 1989.
(21) Eriks, K.; Giering, W. P.; Liu, H.-Y.; Prock, A. *Inorg. Chem.* **1989**, *28*, 1759–1763.
(22) Brodie, N. M. J.; Chen, L.; Poë, A. J. *Int. J. Chem. Kinet.* **1988**, *20*, 467–491.
(23) Bodner, G. M.; May, M. P.; McKinney, L. E. *Inorg. Chem.* **1980**, *19*, 1951–1958.

corresponds to the value of log k_{-CO} for a small ($\theta < \theta_{th}$) and weakly basic ($\delta(^{13}CO) = 0$) ligand.

The data for CO-dissociation from the adduct formed with the 10 smaller nucleophiles[24] give a reasonably good fit to eq 7, and the parameters obtained are shown in Table 6. The values of the RMSD increase steadily as θ_{th} is increased from 101°, so that $\theta_{th} \leq 101°$ and all these reactions are subject to a steric effect, as defined by the value of γ and as shown by the steric profile in Figure 3. The less good fit of data to eq 7,[19] as compared to fits to eq 6, may be ascribed to uncertainties in the precise values of θ,[25] which are more important when the P-donors are present as ligands both in the ground and transition states, rather than simply as partially bonded nucleophiles in the transition states for associative attack.

(d) Stereoelectronic Analysis of Data for Substitution by Larger Nucleophiles. The values of k_2 for larger nucleophiles also fit well to eq 6, with k_{+L} replaced by k_2, and the results are given in Table 6. The RMSD depends on θ_{th} as follows: θ_{th} (RMSD), ≤145° (0.264), 146° (0.206), 147° (0.152), *148° (0.118)*, 149° (0.129), 150° (0.180), 152° (0.272), so that the minimum RMSD is found when $\theta_{th} = 148°$. The change in the RMSD with changing θ_{th} gives a particularly sharp minimum in this case, thus supporting the validity of the existence of the high steric threshold at 148°. Further, the values of log k_2 for nucleophiles 16–19 can be combined with the parameters in Table 6 to predict values for the five nucleophiles with $\theta = 145°$ that are an average of 0.73 ± 0.08 higher than the ones observed, and this suggests that $\theta_{th} \geq 145°$ with a high probability. Although the data analysis and inspection of the steric profile in Figure 4 seem to suggest that the cone angles of the P(p-XC_6H_4)$_3$ nucleophiles (X = H, MeO, Me, Cl, CF_3) only have to be increased to 148° for the steric threshold to disappear, the situation is not as simple as that. If the cone angle for PPh_3 is 148°, then those for PPh_2(i-Pr) and PPh_2Cy would be increased to 152 and 155°, respectively, the slope of the steric profile would increase, and the values of log k_2 for the (now) 148° nucleophiles would still be low. Other evidence for a high steric threshold will be considered in the Discussion section.

The five isosteric nucleophiles P(p-XC_6H_4)$_3$ can be used alone to obtain the value of β. A plot of log k_2 vs pK_a' is shown in Figure 2, and an unweighted linear least-squares analysis gives $\beta = 0.590 \pm 0.036$, $R = 0.995$, and RMSD = 0.150; RMSD/Δlog k_2 = 0.041. The β value obtained in this way is essentially the same as that (Table 6) obtained from data for all the nucleophiles or that (0.51 ± 0.06) obtained from data for only those nucleophiles with $\theta > 145°$.

Discussion

The Stoichiometric Mechanisms. The reactions studied here fall clearly into two types that are distinguished only by the size of the nucleophiles. Those nucleophiles with $\theta \leq 133°$ react to form $Ru_5C(CO)_{14}L$ by two successive steps. These are assignable to adduct formation followed by slower CO loss (eqs 2 and 3), as indicated by the UV–vis and FTIR spectroscopic changes as well as by the linear dependence of k_{obs} on [L] for the first step and the independence of [L] for the second step. The adducts can be assigned structures similar to that of $Ru_5C(CO)_{15}$(NCMe).[4a] Nucleophiles with $\theta \geq 136°$ react instead by a single step to form $Ru_5C(CO)_{14}L$ without any evidence for the intermediate formation of adducts, even at the highest values of [L] used. These qualitative observations show how dramatically the type of reaction can change over a small range of cone angles.[28] The reactions studied kinetically here all involve eventual formation of the monosubstituted products, $Ru_5C(CO)_{14}L$, and the precision of the kinetics (Tables 2–4) is generally excellent.

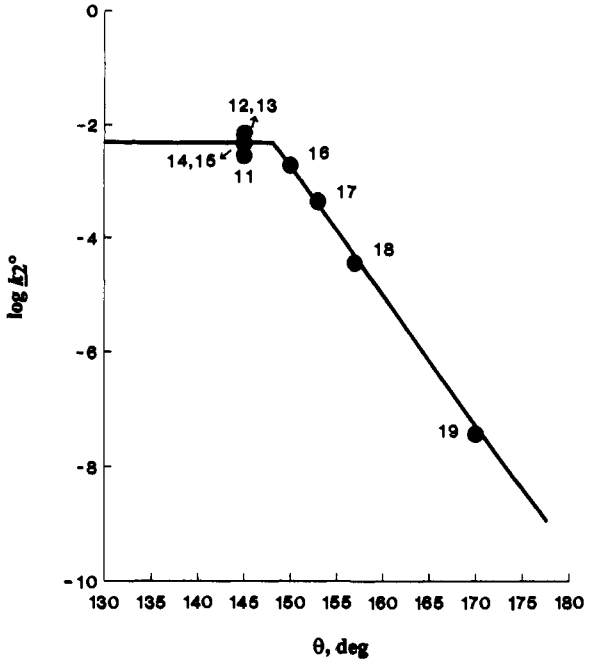

Figure 4. Steric profile for reactions of $Ru_5C(CO)_{15}$ with larger nucleophiles (log k_2° = log $k_2 - \beta(pK_a' + 4)$).

The Intimate Mechanisms. (a) The Distinctiveness of the Two Reaction Paths. The analysis of the data in terms of eq 6 allows the derivation of characteristic parameters that will enable us to assess the intimate mechanisms of the reactions. The behavior is represented graphically by the electronic and steric profiles shown in Figure 2, 3, and 4. The plot of log k ($k = k_{+L}$ or k_2) against pK_a' in Figure 2 shows clearly the very different β values for reactions with the smaller and larger nucleophiles. This difference shows that the two types of reactions cannot both be proceeding by formation of the same sort of adduct, but with the rates of dissociation of CO from adducts with the larger ligands being much faster than their rates of formation (i.e. $k_{-CO} \gg k_{+L}$ in eqs 2 and 3). In this case it would be expected that data for all the nucleophiles would conform to eq 6, with the same value of β. This point can be made more generally by using the kinetic parameters for reactions with one type of nucleophile to calculate what the rates would have been if the reactions of the other type of nucleophile proceeded by the same path. The results of these calculations are shown in Table 7.

In all cases the predicted rates of adduct formation by the larger nucleophiles are as great or greater than the rates actually observed, but the predicted rates of CO-dissociation from those adducts are very much slower than their rates of formation, even at low values of [L]. The fact that adduct formation is not observed can therefore be understood if the adducts, when formed with the larger nucleophiles, are thermodynamically so unstable that the added nucleophile dissociates rapidly to reform the $Ru_5C(CO)_{15}$ cluster; that is, adduct formation is simply a "dead-end reaction" that cannot lead to the product. Conversely, the calculated values of k_2 for reactions of the smaller nucleophiles

(24) Note that k_{-CO}, but not k_{+L}, values were obtained for L = PPh_2(OMe) and PPh_2(OEt).

(25) The question of the validity of the Tolman cone angles for P(OMe)$_3$ and P(OEt)$_3$ and, by inference, all the other ligands that contain OR groups has to be considered in the light of the much larger values that have been proposed.[26] A reconsideration of the data analysis in ref 26, analysis of extensive kinetic data for complexes containing these ligands, and some molecular mechanics calculations have led[27] to an upward adjustment of only 10° for these ligands and, presumably, related increases for other OR-containing ligands. Inspection of the steric profile in Figure 3 shows that such adjustments would have an insignificant effect on it and, in particular, a significant negative gradient would still be shown. The validity of Tolman cone angles for P-donors acting as nucleophiles has been considered briefly in ref 9.

(26) Stahl, L.; Ernst, R. D. *J. Am. Chem. Soc.* **1987**, *109*, 5673–5680.

(27) Chen, L. Ph.D. Thesis, University of Toronto, 1991.

(28) This observation is not unique. Thus, the cluster $Os_3(CO)_9(\mu$-$C_4Ph_4)$[29] reacts with P-donor nucleophiles by [L]-dependent paths to give substitution products $Os_3(CO)_8L(\mu$-$C_4Ph_4)$ when the cone angles of the nucleophiles are ≤143°.[30] Crystallographic analysis of the structure of $Os_3(CO)_8L(\mu$-$C_4Ph_4)$ (L = etpb and P(OPh)$_3$) shows that substitution has occurred at the $Os(CO)_4$ moiety.[31] The [L]-dependent reactions with P-donor nucleophiles of cone angle ≥145° react quite differently via I_N2 fragmentation paths[22] to form the pairs of products $Os(CO)_4L$ and $Os_2(CO)_5L(\mu$-$C_4Ph_4)$, and $Os(CO)_3L_2$ and $Os_2(CO)_6(\mu$-$C_4Ph_4)$.

(29) Ferraris, G.; Gervasis, G. *J. Chem. Soc., Dalton Trans.* **1974**, 1813–1817. Tachikawa, M. T.; Shapley, J. R.; Pierpont, C. G. *J. Am. Chem. Soc.* **1975**, *97*, 7172–7174.

(30) Moreno, C.; Poë, A. J. Unpublished observations.

(31) Farrar, D. H.; Moreno, C.; Poë, A. J.; Ramachandran, R. Unpublished observations.

Table 7. Comparison of Observed Rate Constants with Those Calculated by Assuming that Larger Nucleophiles React by the Paths Followed by Smaller Nucleophiles and that Smaller Nucleophiles React by the Path Followed by Larger Nucleophiles[a]

L	log k_{+L}	log k_{-CO}	log k_2
etpb	**3.468**	**-0.772**	*-0.110*
$P(OMe)_3$	**4.188**	**-0.609**	*0.559*
$P(OEt)_3$	**3.964**	**-1.400**	*1.04*
$PPh(OMe)_2$	**3.814**	**-0.947**	*0.944*
$PPh(OEt)_2$	2.989[b]	**-1.572**	*1.25*
PPh_2H	**3.223**	**-1.524**	*0.376*
$P(OPh)_3$	**2.396**	**-1.421**	*-1.58*
$P(O\text{-}i\text{-}Pr)_3$	**3.553**	**-2.340**	*2.07*
$PPh_2(OMe)$	*3.14*	**-1.419**	*1.31*
$PPh_2(OEt)$	*3.13*	**-2.134**	*1.46*
$P(p\text{-}MeOC_6H_4)_3$	*2.91*	*-2.50*	**2.846**
$P(p\text{-}MeC_6H_4)_3$	*2.77*	*-2.51*	**2.866**
PPh_3	*2.51*	*-2.47*	**2.140**
$P(p\text{-}ClC_6H_4)_3$	*2.00*	*-2.32*	**0.526**
$P(p\text{-}CF_3C_6H_4)_3$	*1.51*	*-2.26*	**-0.785**
$PPh_2(i\text{-}Pr)$	*2.52*	*-2.76*	**2.534**
$PPh_2(Cy)$	*2.52*	*-2.93*	**2.473**
$P(NMe_2)_3$	*2.75*	*-3.21*	**2.781**
PCy_3	*2.52*	*-3.83*	**1.614**

[a] Bold numbers are experimental values, and italicized numbers are the values calculated by using the appropriate parameters from Table 6. [b] This value was obtained experimentally but was omitted when fitting eq 6 (see text).

via the same path as is followed by the larger nucleophiles are found to be uniformly very much smaller (Table 7) than the observed values of k_{+L}. Although these calculations have assumed that θ_{th} for the path followed by the larger nucleophiles is 148°, it can be shown that θ_{th} cannot be much smaller than that. Thus, if θ_{th} = 142°, $P(O\text{-}i\text{-}Pr)_3$ would react via adduct formation and the concerted path at approximately equal rates, and if θ_{th} = 138°, it would react ca. 90% by the latter path. Since there is no evidence that $P(O\text{-}i\text{-}Pr)_3$ reacts at all via the concerted path, it is quite certain that $\theta_{th} \geq 140°$. The free energy profiles for reactions with the two types of ligands can therefore be represented schematically as shown in Figure 5.

(b) The Intimate Mechanism of Adduct Formation. The value of β for adduct formation is quite modest[9,14,22] and suggests that there is only a relatively small degree of bond-making in the transition states. Since there is no reason why the fully formed Ru–P bond in the adduct should be exceptionally weak, this implies a relatively early transition state, which is in accord with the fairly low value of θ_{th} (117°). The low[9] numerical value of γ suggests that the transition state, when formed in the isomeric configuration suitable for attack by these smaller nucleophiles without any steric difficulty,[9] is flexible and easily distorted further so as to accommodate the larger nucleophiles. The value of the SR is the largest observed for associative reactions of over 50 metal carbonyl complexes.[27] It is over 1 order of magnitude larger than that of the next largest ones, which are shown by $Ru_6C(CO)_{17}$[9] and $Rh_4(CO)_{10}(PCy_3)_2$,[9,32,33] and over 6 orders of magnitude larger than that for the reactions of $Ru_3(CO)_{12}$ with smaller nucleophiles (Table 6). The values of β and γ for $Ru_3(CO)_{12}$ and $Ru_5C(CO)_{15}$ are similar, so the extent of bond-making and the flexibility of the transition states are also similar. $Ru_5C(CO)_{15}$, however, has a much higher intrinsic ability to form the transition-state isomer, and this is probably a consequence of its easily distorted, square-based pyramidal configuration[3] coupled with the ability of the C atom to maintain contact with all five Ru atoms during the distortion.

The values of $\Delta H_{+L}^{\ddagger}$ are also in accord with a very facile process, the value for the sterically uninhibited etpb being particularly low and the values for the larger ($\theta > \theta_{th}$) nucleophiles being larger but still low. The increase in $\Delta H_{+L}^{\ddagger}$ along the series from etpb to $PPh(OEt)_2$ is approximately balanced by the increase in $T\Delta S_{+L}^{\ddagger}$ at 298 K. However, the uncertainties in the parameters are sufficiently large that it is not possible to tell whether the values of $\Delta H_{+L}^{\ddagger}$ or $T\Delta S_{+L}^{\ddagger}$ dominate the trend in rates for the particular selection of nucleophiles studied. This raises the important problem that the significance and very existence of parameters obtained by analysis of data according to eq 6 depend on the data being obtained at temperatures that are substantially different from any isokinetic temperature that might possibly apply.

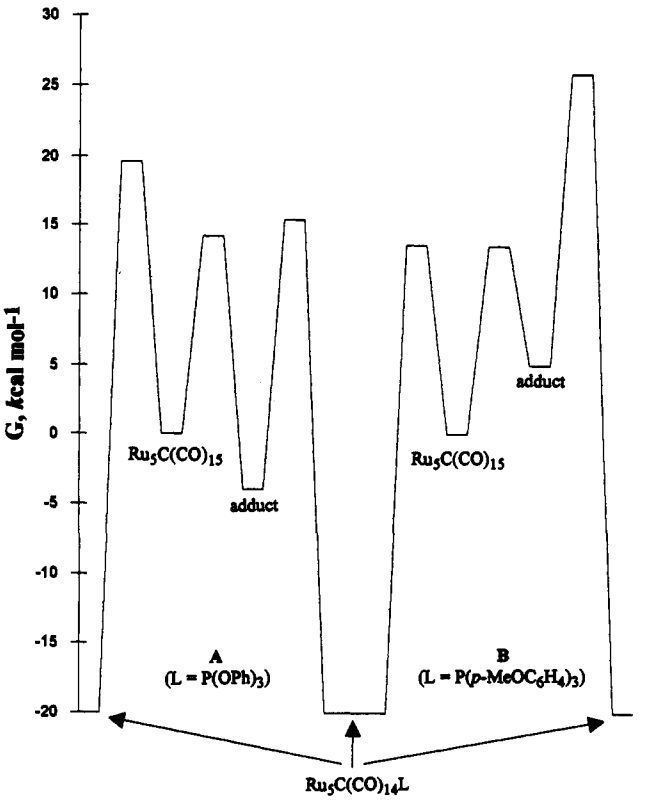

Figure 5. Free energy profiles for reactions of $Ru_5C(CO)_{15}$ with L to form $Ru_5C(CO)_{14}L$. For reactions with L = $P(OPh)_3$ (θ = 128°), A, the barriers for formation of $Ru_5C(CO)_{15}L$ from $Ru_5C(CO)_{15}$, and for loss of CO from $Ru_5C(CO)_{15}L$, are experimental values, while the barrier for the concerted, one-step formation of $Ru_5C(CO)_{14}L$ is the value calculated (from data in Table 7) by using the parameters obtained in Table 6 for reactions with the larger nucleophiles ($\theta \geq 145°$). For reactions with $P(p\text{-}MeOC_6H_4)_3$ (θ = 145°), B, the barrier for the concerted, one-step formation of $Ru_5C(CO)_{14}L$ is the experimental value, while the barriers for formation of $Ru_5C(CO)_{15}L$ from $Ru_5C(CO)_{15}$, and for loss of CO from $Ru_5C(CO)_{15}L$, are the values calculated (from data in Table 7) by using the parameters in Table 6 for reactions with the smaller nucleophiles ($\theta \leq 133°$). The free energies ($\Delta G°$) for formation of the adduct $Ru_5C(CO)_{15}L$ are arbitrarily set to -4 kcal mol^{-1} (L = $P(OPh)_3$, where the adduct is actually formed) and +4 kcal mol^{-1} (L = $P(p\text{-}MeOC_6H_4)_3$, where formation of an adduct is not discernible), while the free energies ($\Delta G°$) for formation of $Ru_5C(CO)_{14}L$ from $Ru_5C(CO)_{15}$ are set arbitrarily at -20 kcal mol^{-1} in both cases.

The process by which adduct formation can be envisaged to occur is illustrated in Scheme 1. The incoming nucleophile is shown as approaching one of the Ru atoms in the basal plane of the Ru_5C cluster from above. This approach is chosen because approach from below can be argued to be both electronically and sterically disfavored by analogy to theoretical and experimental studies of the quite closely analogous clusters $Fe_5C(CO)_{15}$ and $[Fe_5C(CO)_{14}]^{2-}$.[6] Even the H atom is believed to be too large to be bonded to the carbido atom in the basal plane of $Fe_5C(CO)_{15}$, and the molecular orbitals that contain substantial contributions from the carbon atomic orbital in $[Fe_5C(CO)_{14}]^{2-}$ lie sufficiently

(32) Brodie, N. M. J.; Poë, A. J. *J. Organomet. Chem.* **1990**, *383*, 531–542.
(33) Chen, L.; Poë, A. J. *Can. J. Chem.* **1989**, *67*, 1924–1930 and references therein.

Scheme 1[a]

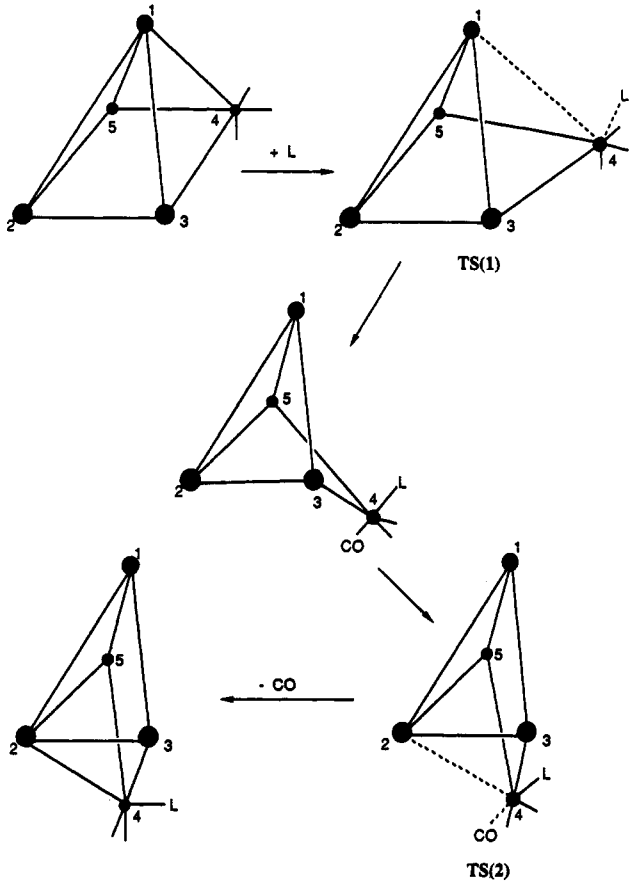

[a] The carbido atoms, and the CO ligands on the Ru atoms not involved directly in the reactions, are omitted for clarity. The CO ligands on Ru(4) are indicated simply by short lines except when CO is the departing ligand. The sizes of the filled circles representing the Ru atoms are varied so as to give some indication of the perspective.

far below the HOMOs for attack by H^+ in the region of the carbido atom to be strongly disfavored. On the other hand, the structure of $Ru_5C(CO)_{15}$ shows clearly[4a] that one of the Ru–Ru "bonds" between the apical and basal Ru atoms is sterically quite accessible to nucleophilic attack by virtue of the particular disposition of the CO ligands around each of the Ru atoms involved. (See Figure 6 in ref 4a, and in particular the positions of the CO ligands labeled 111, 113, 141, and 143 on Ru atoms 11 and 14.)

As the nucleophile approaches Ru(4) in Scheme 1, the Ru(1)–Ru(4) distance increases steadily until the adduct is completely formed, but the carbido atom maintains its connectivity to all five Ru atoms throughout this process, and the structure of the adduct so formed is identical with that found crystallographically for $Ru_5C(CO)_{15}(NCMe)$.[4a] However, although all the $Ru_5C(CO)_{15}X$ adducts including those with X = PPh_2H and $P(OPh)_3$ show rather similar IR bands in solution, those with the P-donors show a number of additional bands. It is possible that isomeric forms of the intermediate butterfly adducts could be formed in solution by fluxional processes or by attack at Ru(4) between the three CO ligands. Postulation of a totally different type of adduct seems unnecessary.

(c) The Intimate Mechanism for Dissociation of CO from the Adducts. The kinetic data for loss of CO from the $Ru_5C(CO)_{15}L$ bridged butterfly adducts are best fitted to eq 7 when there is no steric threshold and the values of β and γ obtained when the data for L = etpb, $P(OMe)_3$, and $P(OEt)_3$ are excluded are essentially the same as when they are included. The value of β is not very well-defined but is almost certainly negative. This implies a stabilization of the ground states, or destabilization of the transition states, by more basic ligands in the adducts. The value of γ is negative, which is unexpected by comparison with the positive values observed[19] for CO-dissociative reactions of mononuclear carbonyls, where the release of steric strain in the transition state leads to positive values of γ. The negative value in this case must imply that the overall bonding within the cluster in the transition state is tighter than in the ground state of the adduct. This is readily understood if formation of the transition state involves an appreciable amount of Ru–Ru bond-making, as is implied in Scheme 1. Similar evidence is provided by the values of $\Delta S_{CO}^{\ddagger}$ (Table 5), which are generally quite negative. Such values have been associated before[33] with tightening up of the residual cluster as a CO ligand leaves and contrast with the positive values observed for dissociative loss of CO from mononuclear carbonyls.

The values of $\Delta H_{CO}^{\ddagger}$ are generally very low compared with CO-dissociation from mononuclear carbonyls such as $Ru(CO)_4L$[19] and from the smaller cluster, $Ru_3(CO)_{12}$.[34] The range of values of $\Delta H_{CO}^{\ddagger}$ and $T\Delta S_{CO}^{\ddagger}$ at 298 K are, respectively, ca. 6 and ca. 8 kcal mol^{-1}, and this suggests that it is the contribution of entropic factors that determines the relative rates of loss of CO from these adducts. Although the values of $\Delta H_{CO}^{\ddagger}$ do change with changing adduct ligand, the values of β and γ obtained at 0 or 50 °C are not significantly different from those at 25 °C when their uncertainties are taken into account.

If the entering nucleophile, in formation of the adducts, enters from above the basal plane, as suggested in Scheme 1, then the loss of CO from the adducts has to be accompanied by formation of a new Ru–Ru bond between the Ru(4) and Ru(2) atoms and the loss of CO from above the developing basal plane defined by Ru atoms (1), (3), (4), and (5). In this way the entering and leaving groups move in and out from above the basal planes, respectively, and the P-donor ligands in the $Ru_5C(CO)_{14}L$ products will occupy an axial position, protruding below the basal plane, as is known from crystallographic structures.[4a,12] The apical Ru atom in the cluster changes from being Ru(1) to Ru(2) during this sequence of reactions, and the rapidity of the overall substitution process must reflect the very high flexibility of the Ru_5C cluster. The carbon atom can maintain contact with all the Ru atoms throughout the substitution process. Formation of an alternative isomeric form of the adduct could allow Ru(4) to return to its original position during CO-dissociation.

(d) The Intimate Mechanism for the Concerted Reactions. The rates of these reactions are governed by a single, second-order rate constant, and there is no spectroscopic indication here of the formation of intermediate adducts. It is still possible for such adducts to be formed provided loss of CO from those adducts is faster than their rate of formation. As has been argued above, however, if adducts are involved, they cannot be the same as those formed with the group of small nucleophiles because loss of CO from such adducts is estimated to be much slower than their rates of formation, so they should be detectable. Although formation of adducts with different structures can be postulated (e.g. by breaking a bond between two Ru atoms in the basal plane of the cluster), there is no evidence for this. The kinetic parameters given by the fit of the data to eq 6 (Table 6) provide some insight into the nature of the transition state.

The value of β for these reactions is the highest value observed so far, only the value (0.55 ± 0.08)[27] for reactions of $Fe(CO)_3(N_4Me_2)$[35] being comparable. This indicates that there is an extremely high degree of bond-making in the transition state. This requires extensive opening of the cluster in forming the transition state ($\theta_{th} = 148°$), and the opened cluster is very resistant to any further opening, as shown by the very large negative value of γ (-0.23 ± 0.01 deg^{-1}), a value only exceeded or approached

(34) Poë, A. J.; Twigg, M. V. *J. Chem. Soc., Dalton Trans.* **1974**, 1860–1866.

(35) Chang, C.-Y.; Johnson, C. E.; Richmond, T. G.; Chen, Y.-T.; Trogler, W. C.; Basolo, F. *Inorg. Chem.* **1981**, *20*, 3167–3172.

by those for $FeCo_2(CO)_9S$ (-0.27 ± 0.06 deg^{-1})[27,36] and $Ru_6C(CO)_{17}$ (-0.20 ± 0.01 deg^{-1}).[9] In the absence of any other evidence we can only conclude that these parameters are the results of a substantial expansion of the Ru_5C cluster that is needed so as to maintain bonding to an increased number of ligands. This is an energetically demanding process that requires an almost compensating contribution of a large amount of energy from Ru–L bond-making. This results in the low value of the intrinsic reactivity that is indicated by the relatively low value of SR and the high value of β. The reasonably low value of $\Delta H_2^{\ddagger}$ for reaction with PPh_3 (Table 5) shows that the extensive bond-making does lower the overall enthalpy needed to form the transition state quite effectively in this case. The unexceptional value of $\Delta S_2^{\ddagger}$ suggests that any severe limitation on the path of approach of the nucleophile is probably offset by the extensive loosening of the bonding within the Ru_5C cluster.

The existence of two paths for nucleophilic attack on this cluster is not unique. Recent studies of associative reactions of the archetypal carbonyl cluster $Ru_3(CO)_{12}$ have shown[27,37] that reactions with smaller nucleophiles ($\theta \leq 136°$) proceed (Table 6) with a β value of 0.16 ± 0.03, while reactions with the isosteric nucleophiles $P(p\text{-}XC_6H_4)_3$ ($\theta = 145°$) are governed by a significantly larger value of β (0.35 ± 0.01).

Summary

These very detailed studies of the kinetics of substitution reactions of the HNCC $Ru_5C(CO)_{15}$ with P-donor nucleophiles enable us to come to the following conclusions.

(1) The reaction paths for the overall substitution reactions are dominated by steric effects. Reactions with smaller nucleophiles ($\theta \leq 133°$) proceed via rapid formation of bridged butterfly adducts similar to those that have been structurally characterized.[4a] Reactions with larger nucleophiles ($\theta \geq 136°$) proceed via a quite different path with no detectable intermediates. Similarly dramatic dependence of reaction paths on the precise size of the nucleophiles has been observed in this laboratory for other systems.[28,37]

(2) The kinetic parameters for adduct formation with the group of smaller nucleophiles suggest that the reaction has an early transition state. The intrinsic readiness of the cluster to undergo the structural changes necessary to form the transition states is exceptionally high.

(3) The kinetic parameters obtained from the dependence of the rates of CO dissociation from the adducts show that there is a significant contribution of Ru–Ru bond-making in the transition states which are destabilized, with respect to the ground-state adducts, by more basic ligands. The Ru–Ru bond formation becomes more difficult as the size of the ligands in the adducts increases.

(4) Reaction with the group of larger nucleophiles proceeds via only one observable transition state. The kinetic parameters show clearly that a major expansion of the Ru_5C cluster has to occur in forming the transition state, and this requires an exceptionally high degree of Ru–nucleophile bond-making for it to be possible. Further distortion of the transition state by the larger of the group of large nucleophiles is also exceptionally difficult.

(5) These detailed conclusions about the stoichiometric and intimate mechanisms of these apparently simple substitution reactions could only have been obtained by extensive and detailed studies of the dependence of the natures and rates of the reactions on the electronic and steric properties of the entering P-donor ligands.

Acknowledgment is made to the donors of the Petroleum Research Fund, administered by the American Chemical Society, for partial support of the research, to the University of Toronto for the award of an Open Fellowship (to Y.Z.), and to the reviewers for helpfully critical comments.

Supplementary Material Available: Tables of FTIR data and values of k_{obs} (9 pages). This material is contained in many libraries on microfiche, immediately follows this article in the microfilm version of the journal, and can be ordered from the ACS; see any current masthead-page for ordering information.

(36) Data from the following: Rossetti, R.; Gervasio, G.; Stanghellini, P. L. *J. Chem. Soc., Dalton Trans.* **1978**, 222–227.

(37) Chen, H.; Chen, L.; Poë, A. J. Unpublished results.